

Ultrafast demagnetization dynamics of thin Fe/W(110) films: Comparison of time- and spin-resolved photoemission with time-resolved magneto-optic experiments

A. Weber,¹ F. Pressacco,¹ S. Günther,¹ E. Mancini,^{1,*} P. M. Oppeneer,² and C. H. Back¹

¹*Institut für Experimentelle und Angewandte Physik, Universität Regensburg, Universitätsstrasse 31, D-93040 Regensburg, Germany*

²*Department of Physics and Astronomy, Uppsala University, Box 516, SE-75120 Uppsala, Sweden*

(Received 16 August 2011; revised manuscript received 24 September 2011; published 20 October 2011)

We report the results of time- and spin-resolved photoemission (TR-SPES) and time-resolved magneto-optical Kerr effect experiments on iron thin films. In particular, the extracted demagnetization times for both techniques are compared. It is shown that while for the Kerr measurements the demagnetization times are always limited by our time resolution (250 ± 30 fs), for the TR-SPES measurements this situation occurs only for relative quenching below 30%. Above this value, the measured TR-SPES demagnetization time exceeds 500 fs. Different demagnetization probes can hence track different demagnetization times.

DOI: [10.1103/PhysRevB.84.132412](https://doi.org/10.1103/PhysRevB.84.132412)

PACS number(s): 75.78.Jp, 75.70.-i, 78.20.Ls, 78.47.-p

Since the discovery of ultrafast demagnetization in Ni films by Beaupaire *et al.* in 1996,¹ various experiments have addressed the validity of the quenching of the magnetization on a sub-100-fs time scale.² While the origin of the time-resolved magneto-optical Kerr effect (TR-MOKE) signal in the femtosecond regime was the subject of intense debate,³ over the years the existence of ultrafast demagnetization has been unambiguously established. In fact, ultrafast demagnetization has been observed in all ferromagnetic $3d$ transition metals and some of their alloys, as well as the elementary $4f$ elements Gd and Tb and some $3d$ - $4f$ alloys. In addition, ultrafast demagnetization has also been verified by various approaches ranging from time-resolved nonlinear optical methods to time-resolved electron spectroscopies, such as time-resolved photoemission,^{4,5} time-resolved two-photon photoemission,⁶ time-resolved spin-polarized photoemission (TR-SPES),⁷ and second-harmonic generation (SHG).⁸ Recently, time-resolved x-ray magnetic circular dichroism (TR-XMCD)⁹⁻¹² experiments as well as tabletop magnetic linear dichroism experiments in the XUV range¹³ have also unambiguously proven the quenching of the magnetization on an ultrafast time scale. Although ultrafast demagnetization has been experimentally established, there is still no general consensus about the microscopic mechanisms responsible for the quenching of the angular momentum of the magnetic material and the conservation of the total angular momentum, calling for further experimental and theoretical efforts.

On the theory side, various models exist in various levels of complication ranging from the purely phenomenological three-temperature model (3TM), which neglects angular momentum completely,¹ to atomistic calculations,¹⁴ microscopic models based on Elliott-Yafet type phonon scattering,^{15,16} superdiffusive transport process,¹⁷ and magnon generation by hot electrons.¹⁸ So far, none of these models can realistically predict the evolution of spin and orbital moment as a function of time in real solids (in the model of Zhang and Hübner,¹⁹ where the role of the transfer of moment between the spin and the orbital degree of freedom has been addressed, the angular momentum of the lattice has been neglected). In a recent paper, a universal picture to reconcile some of the observed demagnetization times has been put forward. Koopmans *et al.* combine a simplified Elliott-Yafet-type theory with *ab*

initio calculations to explain the demagnetization experiments performed using optical methods at various laser fluences for Ni and Co, as well as TR-XMCD-based experiments on Gd. However, the simple model seems to fail to capture the results obtained on Tb.¹²

Thus, it would be desirable from an experimental point of view to test ultrafast demagnetization with complementary methods. One method to selectively probe the temporal evolution of the spin polarization has already been demonstrated in 1997. Scholl *et al.*⁷ showed that TR-SPES is able to follow the temporal evolution of the spin polarization of thin Ni films. However, their experiments exhibiting two time scales for the quenching of the magnetization were never understood theoretically and have not been reproduced so far.

In this Brief Report, we use two complementary experimental approaches to probe ultrafast magnetization dynamics. We demagnetize 8 monolayer (ML) thin Fe films epitaxially grown on W(110) using a 1.48 eV pump laser pulse. We probe the temporal evolution of the magnetization using TR-MOKE at a probe photon energy of 2.95 eV. In addition (in some cases on the exact same film), we use TR-SPES to probe the evolution of the spin polarization of the film (exciting photon energy 5.9 eV). Interestingly, we observe *different* time scales at high laser fluences for the demagnetization process with the demagnetization time in TR-SPES being significantly longer than the one in TR-MOKE.

The experiments are performed in an ultrahigh vacuum system equipped with preparation and measurement chambers. The W(110) single crystal is prepared by heating it to 1000 K in a 2×10^{-6} mbar of oxygen partial pressure (base pressure 1×10^{-10} mbar) for 20 min followed by flashing cycles to 2100 K for 10 s, until no traces of carbon and oxygen can be detected using Auger electron spectroscopy (AES). Subsequently, Fe thin films are evaporated at room temperature onto the clean substrate using molecular-beam epitaxy from tungsten crucibles using electron-beam heating at a rate of 0.2 ML/min. The pressure during deposition does not exceed 4×10^{-10} mbar. The thickness of the films is monitored using a quartz microbalance calibrated using AES. The crystalline quality is monitored using low-energy electron diffraction and the chemical quality using AES. The magnetic easy axis of the Fe films coincides with the $[1\bar{1}0]$ direction. Hysteresis loops

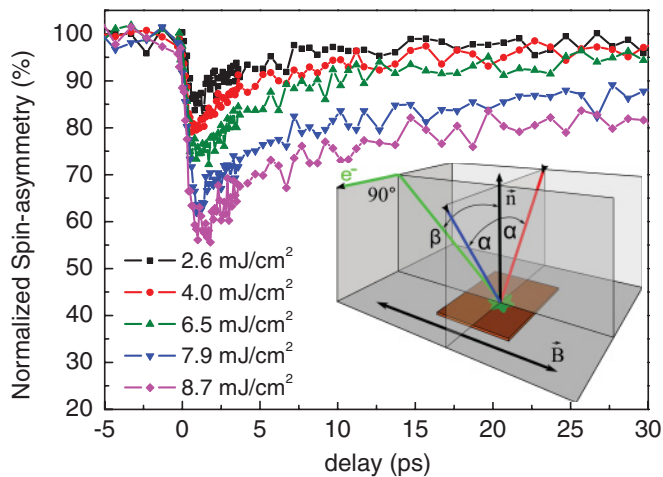


FIG. 1. (Color online) Normalized spin asymmetry for different incident pump fluences. The 100% polarization for negative delays corresponds to an actual spin asymmetry of $27.1 \pm 1.3\%$. Inset: Schematic representation of the experimental geometry for the spin-resolved photoemission.

measured using the static magneto-optic Kerr effect show a coercive field of about 30 Oe for all films prepared and a square loop shape with 100% remanence. Some of the films are capped with 25-ML-thick Ag films and are measured also *ex situ* using TR-MOKE. Capping leads to an increase of the coercivity to ≈ 100 Oe.

The freshly prepared films are transferred to the measurement chamber (base pressure in 6×10^{-11} mbar), where we perform TR-MOKE and TR-SPES experiments. The photon source is a cw-pumped Ti:Sapphire regenerative amplifier delivering pulse trains at a repetition rate between 25 and 76 kHz at a wavelength of 840 nm (from now on labeled IR, 1.48 eV). The repetition rate is chosen such that no dc heating of the sample is observed, while guaranteeing a high incident fluence of the fundamental pump beam of up to 13 mJ/cm² measured at the sample position. The fundamental IR beam is frequency doubled in two doubling stages. The frequency-doubled beam (from now on labeled blue, 420 nm, 2.95 eV) is used as a probe pulse for the TR-MOKE experiments, while the frequency-quadrupled beam (from now on labeled UV, 210 nm, 5.9 eV) is used to excite threshold photoelectrons in a one-photon photoemission process for the TR-SPES experiments. Both blue and UV beams are focused onto the sample through the same achromatic objective lens at an angle of $\alpha = 30^\circ$ with respect to the surface normal; see Fig. 1. The resulting spot sizes on the sample are $30 \mu\text{m}$ in diameter for the blue and UV beams. The reflected blue beam is collected through a second achromatic lens and directed into a Wollaston prism setup with a balanced photodetector for TR-MOKE experiments in the longitudinal geometry. After delaying the fundamental IR beam via an optical delay line, it is focused onto the sample through the same achromatic objective lens which is used for collecting the blue light. Its spot diameter is $60 \mu\text{m}$. For the experiments shown in the following, the IR is *p* polarized, while the polarization of the blue and UV beams is set to 45° with respect to the scattering plane. A small coil in the measurement position allows reversing the magnetization of the films with magnetic fields up to 120 Oe. The excited

photoelectrons are collected using an electrostatic lens system at $\beta = 45^\circ$; see Fig. 1. They are subsequently sent through a 90° deflector, which allows us to measure simultaneously the out-of-plane component of the spin polarization as well as the in-plane component perpendicular to the photon-scattering plane. The spin polarization of the photoelectrons is analyzed in a standard 40 kV Mott detector described elsewhere.²⁰ For each point in time, we record the scattering asymmetry for both magnetic field directions and determine the value of the spin polarization. For the longitudinal TR-MOKE measurements, we turn the sample and the magnetic field coils by 90° . For the experiments described below, it is important to determine the pulse duration of the laser pulses of different photon energies. The pulse duration of the IR pulse is determined to be 250 ± 30 fs using an autocorrelator. To determine the pulse length of the blue beam, we use two-photon photoemission from the clean tungsten single crystal in the sample position and also obtain a value of 250 fs. We note at this point that we do not observe any increase in the number of electrons from multiphoton photoemission in our experiments when the pump beam hits the sample. In fact, the electron count rate remains exactly the same for all measurement times, except for the temporal overlap of pump and probe beams where we observe a 5% decrease of count rate. A change in count rate at the pump-probe overlap has been observed before and can be used to estimate the pulse length of the UV pulse. We determine a value of 350 ± 50 fs. The time resolution is only weakly declined due to the relative angle of 60° between the pump and probe pulses.

Figure 1 shows the normalized spin polarization as a function of time delay between the pump and probe pulses for several fluences. First, we observe a relative drop of the spin polarization (up to 45%) from its initial value of $27.1 \pm 1.3\%$ measured for the unperturbed film. Second, a minimum in the spin polarization is observed after about 1 ps, followed by a recovery on a time scale of a few picoseconds. We note here that we do not observe the two-step demagnetization behavior observed by Scholl *et al.*⁷ In fact, the spin polarization recovers to its initial value for all applied fluences on time scales between 30 to some hundreds of ps depending on the incident fluence. The relative quenching of the spin polarization is a linear function of the pump fluence with a slope of $4.5\% \text{ mJ}^{-1} \text{ cm}^2$. The behavior is linear over the fluence interval studied here and we conclude that we are still reasonably far away from the Curie temperature of the Fe films studied here.

In order to retrieve the characteristic time constants for the demagnetization and remagnetization processes, we use the phenomenological fit function^{21,22}

$$f(t) = H(t) \left[A \left(1 - e^{-\frac{t}{\tau_M}} \right) e^{-\frac{t}{\tau_R}} \right].$$

Here $H(t)$ is the step function, τ_M and τ_R are demagnetization and remagnetization time constants, respectively, and A is the exponential amplitude. Convolution with the laser-pulse duration results only in minor corrections of the extracted demagnetization times.

We performed additional TR-MOKE measurements *ex situ* in order to increase the signal-to-noise ratio. For this purpose, we used prepared Ag capped films with identical thickness.

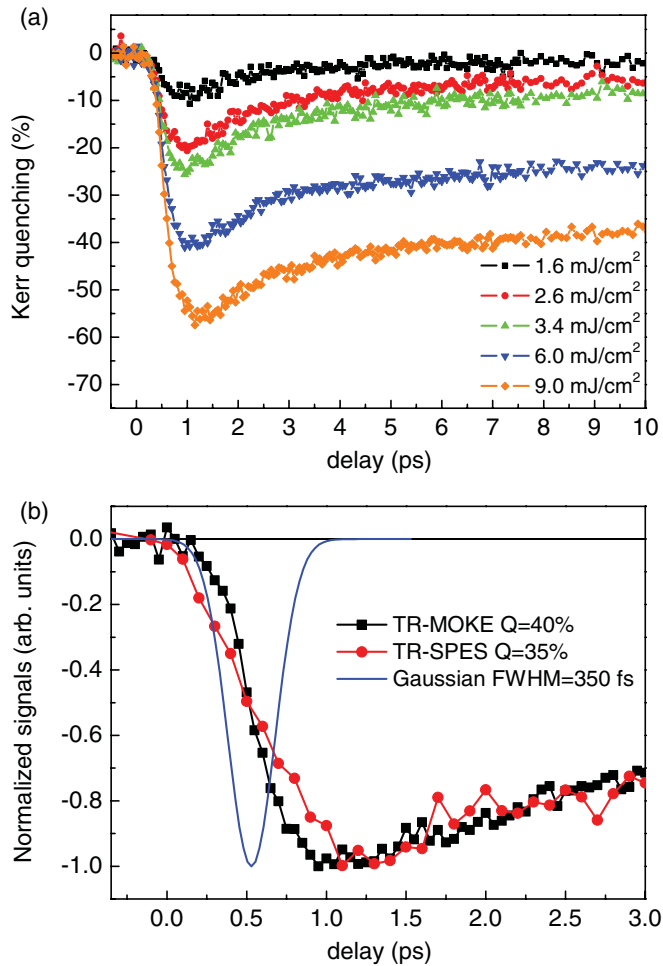


FIG. 2. (Color online) (a) TR-MOKE curves for different fluences. (b) Comparison between the TR-SPES ($Q = 35\%$) and TR-MOKE ($Q = 40\%$) responses. The blue solid line represents the time resolution in the photoemission experiment (350 ± 50 fs).

The Kerr measurements are reported in Fig. 2(a). The relative quenching varies from 10% to 55% scaling linearly with the pump fluence (not shown). In Fig. 2(b), we compare the normalized TR-SPES and TR-MOKE responses for similar quenching. As can be noticed, the demagnetization curves in the two cases have different character. A clear difference in the demagnetization time is visible while the remagnetization traces after about 1 ps fall roughly on one curve. At longer time scales, slight differences in the remagnetization times might arise from the use of a capping layer in the case of the TR-MOKE experiments; see inset in Fig. 3. In the Kerr data, the demagnetization time τ_M is limited by the time resolution (250 ± 30 fs), while for the photoemission experiment, τ_M is longer than the corresponding temporal probing resolution (350 ± 50 fs) represented by the Gaussian curve shown for comparison in Fig. 2(b).

The most interesting results from the comparison of the TR-MOKE and TR-SPES data are summarized in Fig. 3. Here we plot the demagnetization and remagnetization times extracted from TR-SPES (squares) and TR-MOKE (circles) as a function of relative quenching. In this way, we can avoid artifacts due to the different reflectivities and thus of different absorbed

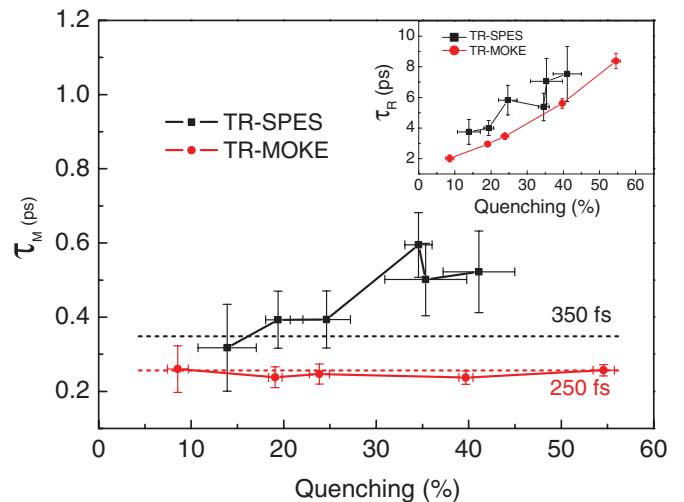


FIG. 3. (Color online) The extracted demagnetization times for TR-SPES and TR-MOKE measurements. The Kerr data are limited by the laser-pulse length. The photoemission data are limited by the pulse duration only for relative quenching $\leq 30\%$, while above this percentage, their value is ~ 500 fs. The black (upper) and red (lower) dashed lines represent the TR-SPES and TR-MOKE time resolutions, respectively. Inset: Initial remagnetization times for both measurements.

fluences of the samples. For TR-SPES experiments, the relative quenching can be directly obtained from the measured spin polarization, which is an absolute signal. For TR-MOKE experiments, we have measured additional hysteresis loops for the time of maximum quenching to normalize the signal. In contrast to the results of Ref. 23 measured on thin Fe/MgO(100) films using TR-MOKE, we find a constant demagnetization time of about 250 fs for all the fluences. Carpené *et al.* observe much shorter demagnetization times in their experiments (between 50 and 75 fs) for comparable fluences between 1.5 and 6 mJ/cm². However, it should be noted that the time resolution in the present experiment is essentially the same as the measured τ_M and is given by the laser-pulse duration. In the case of TR-SPES experiments, however, even with the big error bars²⁴ and the poorer time resolution (350 ± 50 fs), a quenching dependence is still visible. Indeed, we see that the low fluence points are dominated by the pulse length of the UV pulses, while for higher fluences, we obtain demagnetization times around 500 fs.

The obtained results call for an investigation of the origin of the measured demagnetization differences. Obviously, both TR-MOKE and TR-SPES are probes of the magnetization and hence are expected to detect an *identical* demagnetization. Such behavior is seen at time delays above 1 ps, in the remagnetization regime where the electrons have thermalized, but not in the demagnetization regime. A major question is where such a difference may arise from, as the existence of absolute demagnetization times is an essential assumption in the ongoing discussion regarding the microscopic ultrafast mechanism.

By analyzing the differences between the experiments, a first distinction noted is the probe pulse energy. In TR-MOKE, we probe transitions at an energy of 2.95 eV; all possible transitions within the Brillouin zone (BZ) contribute to the

MOKE signal.^{25,26} For the TR-SPES data, photoelectrons are excited by the 5.9 eV probe pulse. Due to energy and k -vector conservation, and the work function of Fe $\Phi = 4.5$ eV, only photoelectrons within a narrow region around the $\Gamma - \Sigma - N$ direction in the BZ are emitted from the crystal surface ($|\mathbf{k}_{\max}| = 0.606 \text{ \AA}^{-1}$). Thus, the two techniques probe the transient behavior of distinct spin-polarized states in the BZ.

A second possible origin could be that state-blocking effects³ influence the apparent demagnetization of the probed band states. TR-MOKE is expected to be affected more, as it probes unoccupied states in reach of the IR pump beam. The pulse durations used here are, however, relatively long, therefore one expects that initial state-blocking effects have diminished, as fast electron-electron scattering has already reduced the nonequilibrium electron distribution.²⁶

A third possible source of differences is the possible influence of the Ag cap layer on the demagnetization. In this case, so-called superdiffusive transport of carriers after excitation in Ag can contribute additionally to the quenching of the magnetization in Fe.¹⁷ Conversely, superdiffusive spin transport from the Fe into the Ag layer removes hot carriers from the Fe. Detailed calculations would be needed to establish how much these contributions compensate. As we extract here the TR-SPES and TR-MOKE demagnetization times relative to the quenching, the influence of the superdiffusive contributions from and to the Ag cap layer is likely not large enough to explain the different demagnetization times.

Finally, we would like to mention that a possible origin for our observations can be attributed to the underlying fact that magneto-optics probe the magnetization via spin-orbit coupling, while the photoemission experiment analyzes directly the spin polarization of the electrons, which is primarily responsible for the magnetic order in transition metals. Exchange interaction and spin-orbit interaction may impose different time scales on the demagnetization process. Since magnetic order in $3d$ transition metals is mostly composed of the electron spin, the observed time scales may be the relevant ones for ultrafast demagnetization of the macroscopic

magnetization. In fact, recently two TR-XMCD experiments on Ni (Ref. 9) and CoPd (Ref. 10) films reported some interesting results. Whereas in thin Ni films, it has been observed that the quenching of the angular and spin moment take place on similar time scales, in the case of CoPd films (having strong perpendicular anisotropy), the z component of the spin moment seems to respond more slowly than the corresponding z component of the orbital component.

Our results point to distinct demagnetization times existing for different band states within the BZ or different experimental probes (via spin-orbit interaction or spin polarization). This finding raises the question of the validity of TR-MOKE and TR-SPES data in general. Only photoemission experiments, where all photoelectrons contributing to the spin imbalance are emitted and spin analyzed, would be a true measure of the spin polarization of a sample. This requires a much higher photon energy (at least of the order of the band width of the d -electron band plus the work function) for photoelectron emission. Similar arguments hold for MOKE experiments. While relative comparisons can be made for all optical pump-probe experiments in the IR-to-visible energy range (e.g., comparison of the evolution of the demagnetization time as a function of fluence for a particular choice of pump and probe energy), a true measure of the demagnetization time can consequently most likely only be performed for magneto-optic probe pulses in the soft x-ray regime.⁹⁻¹²

In summary, we have performed two complementary time-resolved experiments on ultrathin Fe films, revealing demagnetization times in the subpicosecond regime. In particular, at high laser fluences, a different demagnetization response is observed in the two approaches. The experiments show the need for development of microscopic theories tracking the response of individual band states.

We would like to acknowledge fruitful discussions with H.A. Dürr, G. Woltersdorf, M. Battiato, and K. Carva. Financial support from the European Union through the FP7-ITN “FANTOMAS” project is gratefully acknowledged.

*eduardo.mancini@physik.uni-regensburg.de

¹E. Beaurepaire, J. C. Merle, A. Daunois, and J. Y. Bigot, *Phys. Rev. Lett.* **76**, 4250 (1996).

²A. Kirilyuk, A. Kimel, and T. Rasing, *Rev. Mod. Phys.* **82**, 2731 (2010).

³B. Koopmans, M. vanKampen, J. T. Kohlhepp, and W. J. M. deJonge, *Phys. Rev. Lett.* **85**, 844 (2000).

⁴H. S. Rhie, H. A. Dürr, and W. Eberhardt, *Phys. Rev. Lett.* **90**, 247201 (2003).

⁵M. Lisowski, P. A. Loukakos, A. Melnikov, I. Radu, L. Ungureanu, M. Wolf, and U. Bovensiepen, *Phys. Rev. Lett.* **95**, 137402 (2005).

⁶M. Cinchetti, M. SanchezAlbaneda, D. Hoffmann, T. Roth, J. P. Wustenberg, M. Krauss, O. Andreyev, H. C. Schneider, M. Bauer, and M. Aeschlimann, *Phys. Rev. Lett.* **97**, 177201 (2006).

⁷A. Scholl, L. Baumgarten, R. Jacquemin, and W. Eberhardt, *Phys. Rev. Lett.* **79**, 5146 (1997).

⁸H. Regensburger, R. Vollmer, and J. Kirschner, *Phys. Rev. B* **61**, 14716 (2000).

⁹C. Stamm *et al.*, *Nature Mater.* **6**, 740 (2007).

¹⁰C. Boeglin *et al.*, *Nature (London)* **465**, 458 (2010).

¹¹I. Radu *et al.*, *Nature (London)* **472**, 205 (2011).

¹²M. Wietstruk, A. Melnikov, C. Stamm, T. Kachel, N. Pontius, M. Sultan, C. Gahl, M. Weinelt, H. A. Dürr, and U. Bovensiepen, *Phys. Rev. Lett.* **106**, 127401 (2011).

¹³C. La-O-Vorakiat *et al.*, *Phys. Rev. Lett.* **103**, 257402 (2009).

¹⁴N. Kazantseva *et al.*, *Europhys. Lett.* **81**, 27004 (2008).

¹⁵B. Koopmans *et al.*, *Nature Mater.* **9**, 259 (2009).

¹⁶B. Koopmans, J. J. M. Ruigrok, F. DallaLunga, and W. J. M. deJonge, *Phys. Rev. Lett.* **95**, 267207 (2005).

¹⁷M. Battiato, K. Carva, and P. M. Oppeneer, *Phys. Rev. Lett.* **105**, 027203 (2010).

¹⁸A. Schmidt, M. Pickel, M. Donath, P. Buczek, A. Ernst, V. P. Zhukov, P. M. Echenique, L. M. Sandratskii, E. V. Chulkov, and M. Weinelt, *Phys. Rev. Lett.* **105**, 197401 (2010).

¹⁹G. P. Zhang and W. Hübner, *Phys. Rev. Lett.* **85**, 3025 (2000).

²⁰V. Petrov *et al.*, *Rev. Sci. Instrum.* **74**, 1278 (2003).

- ²¹L. Guidoni, E. Beaurepaire, and J. Y. Bigot, *Phys. Rev. Lett.* **89**, 17401 (2002).
- ²²N. Del Fatti, C. Voisin, M. Achermann, S. Tzortzakis, D. Christofilos, and F. Vallee, *Phys. Rev. B* **61**, 16956 (2000).
- ²³E. Carpenne, E. Mancini, C. Dallera, M. Brenna, E. Puppini, and S. DeSilvestri, *Phys. Rev. B* **78**, 174422 (2008).
- ²⁴All the reported error bars correspond to the uncertainties obtained from the fitting procedure.
- ²⁵P. M. Oppeneer, T. Maurer, J. Sticht, and J. Kubler, *Phys. Rev. B* **45**, 10924 (1992).
- ²⁶P. M. Oppeneer and A. Liebsch, *J. Phys. Condens. Matter* **16**, 5519 (2004).